Electronic structure and lattice distortions in $PbMg_{1/3}Nb_{2/3}O_3$ studied with density functional theory using the linearized augmented plane-wave method

Malliga Suewattana[1,2] and David J. Singh[1]
[1]*Materials Science and Technology Division, Oak Ridge National Laboratory, Oak Ridge, Tennessee 37831, USA*
[2]*Department of Physics, University of Tennessee, Knoxville, Tennessee 37996, USA*
(Received 3 March 2006; published 7 June 2006)

We investigated the local structural distortions of PMN($PbMg_{1/3}Nb_{2/3}O_3$) within the density functional theory using the linearized augmented plane-wave method. Structural relaxations were performed on 30 atom unit cells with *B*-cations arranged in 1:1 chemical ordering along [111]. The direction and magnitude of Mg and Nb off-centering within O_6 octahedral cages and Pb within its cage as well as electronic structures were examined. The results are discussed in terms of the Nb 4*d*-O 2*p* and Pb 6*p*-O 2*p* hybridizations and their interplay. A significant role is found for the on-site Ewald potential of different Nb sublattices, which is correlated with the off-centering.

DOI: 10.1103/PhysRevB.73.224105 PACS number(s): 77.84.Dy, 71.15.Nc

I. INTRODUCTION

Perovskite structure $Pb(Mg_{1/3}Nb_{2/3})O_3$ (PMN) is of interest both as a prototypical Pb containing relaxor ferroelectric[1] and as the end point of the high coupling piezoelectric crystal alloy $Pb(Mg_{1/3}Nb_{2/3})O_3$-$PbTiO_3$ (PMN-PT).[2,3] While ferroelectricity in Pb containing perovskites, ABO_3, A=Pb, is driven primarily by the stereochemical activity of Pb, the *B*-site ions play an important role both in the production of the morphotropic phase boundaries and facile polarization rotation that underlies piezoelectric performance[4] and in providing the disorder that leads to relaxor ferroelectricity.[5–10] In PMN, the disorder is associated with the disorder between Mg^{2+} and Nb^{5+} on the perovskite *B*-site. However, the details of the interplay between local chemical environment, the ferroelectric activity of Pb, and the *B*-site ions, and the relaxor behavior is not fully understood.

Several first principles studies of the structural and dynamical behavior in supercells have been performed.[11–13] Prosandeev and co-workers,[12] and Choudhury and co-workers[13] investigated several different orderings using supercells and found significant differences in the vibrational spectra depending on the particular *B*-site ordering. From a microscopic point of view, the physics of these materials is complex. Instabilities of perovskites can often be understood in terms of ionic size effects, especially in terms of tolerance factors.[14] In addition, both *A*-site-O and *B*-site-O hybridization are important in polar instabilities of Pb containing perovskites.[15] The polar modes, and modes that compete with them are highly sensitive to strain, which in turn can vary depending on local chemical ordering.[16,17] The interaction between polar off-centerings on different cation sites has been shown to be complex involving both dipolar interactions and short range interactions that can be understood in terms of bond competitions with O.[11]

II. APPROACH

Here we use supercell calculations to investigate the interplay between variations in electrostatic potentials, *B*-site hybridization, and polar distortions in PMN. The motivation comes from the fact that, while in Pb containing perovskites polar behavior is driven by the *A*-site, and the *B*-site plays a role in stabilizing the ferroelectricity and in selecting the direction of polarization (e.g., [111] vs [001]).[18] In any alloy containing 5+ and 2+ ions, one may expect variations in the local electrostatic potential, perhaps by tenths of eV, due to different local coordinations. Such changes can affect *B*-site hybridization by changing the gap between the O 2*p* valence bands and the unoccupied metal *d* bands. For example, $KNbO_3$ shows robust *B*-site driven ferroelectricity, while $KTaO_3$ is not ferroelectric, even though the ionic radii and lattice parameters are almost identical—the difference is due to a $\sim 1/2$ eV larger band gap in $KTaO_3$ with the result that the *B*-O hybridization is weaker in $KTaO_3$ than in $KNbO_3$.[19] Although $KNbO_3$ is *B*-site driven and PMN is *A*-site driven, the peak in the temperature dependent dielectric response of $Pb(Mg_{1/3}Ta_{2/3})O_3$ is $\sim$80 K lower than in PMN, likewise indicating a role for Nb-O covalency.

The calculations were done within the local density approximation (LDA) using the general potential linearized augmented planewave (LAPW) method.[20,21] This is an all electron method, in which the full crystal potential is used. As such, core states are calculated self-consistently in the same potential as the valence states. This allows us to characterize the site-dependent changes in the on-site potential using the positions of inner core levels, e.g., the 1*s* level. Local orbital extensions were used to relax linearization errors and to treat the semicore states. Specifically, local orbitals were used for the Pb 5*d*, Mg 2*p*, Nb 4*s*, and Nb 4*p* semicore states and to relax linearization errors for the Nb *d* and O *s* and *p* channels. LAPW sphere radii of 2.1, 1.85, 1.85, and 1.50 a.u. were used for Pb, Mg, Nb, and O, respectively. We used converged basis sets obtained with a LAPW cutoff $RK_{max}=7$, where $R=1.50$ a.u., is the radius of the smallest LAPW sphere (O in this case). Zone sampling was done using the standard Monkhorst-Pack special **k**-points method[22] with (2,2,2) meshes. Relaxations were done using the calculated forces and were stopped when the forces reached the level of 0.002 Ry/a_0. We crosschecked our results against calculations with the WIEN2K (Ref. 23) code using the augmented planewave plus local orbital method[24]

with different sphere radii, and also checked different **k**-points sampling, but found changes in the forces below 0.002 Ry/a_0, which is not significant. In general, the LDA is thought to be more reliable than the GGA for determining the structures of Pb containing ferroelectrics, especially when experimental lattice parameters are used.[25] Crystal structure predictions born out by subsequent experiments and excellent agreement with modern neutron diffraction has been obtained for $PbZrO_3$,[26] and piezoelectric and other properties of $PbTiO_3$ are well described.[15,27] However, we calculated the forces for our relaxed LDA structure within the generalized gradient approximation of Perdew, Becke, and Ernzerhof,[28] but found only small forces. The maximum and r.m.s. average forces were small: 0.014 Ry/a_0 and 0.010 Ry/a_0, respectively.

III. LATTICE STRUCTURES

We did calculations for two supercells: (1) a 30 atom cell based on a 1:1 ordering (related to the random-site model, but with a specific ordering on the mixed sublattice), consisting of a NaCl ordering of two sublattices, the first of Nb and the second of composition $Mg_{2/3}Nb_{1/3}$ with layering of Mg and Nb in (111) planes on the mixed sublattice, and (2) a minimal 15 atom cell based on 1:2 ordering constructed by tripling the simple cubic perovskite cell, which yields a stacking ···Mg-Nb-Nb-Mg-Nb··· along the (001) direction. Most of the discussion here is based on the results for the 1:1, 30 atom cell, which is shown in Fig. 1. In both cases, the lattice parameters were held fixed at the experimental cubic lattice parameter of PMN, 4.049 Å.[29] These two cells were chosen because they both have local charge neutrality and because there is evidence that the inhomogeneity in PMN that underlies the formation of polar nanoregions may be variations in the amount of 1:1 order.[5,10] When fully relaxed, we found that the 30-atom 1:1 supercell had a 0.20 eV per formula unit lower in energy than the 1:2 cell. This is in agreement with the conclusions of Prosandeev and co-workers.[12]

We briefly discuss the relaxed structure before turning to the electronic properties. The relaxed structures for the 1:1 cell is polar, while the (001) stacked cell has an antiferroelectric ground state in which Pb atoms sandwiched between Nb and Mg layers strongly off-centered towards the Mg as would be expected both from electrostatic and bond competition considerations. This is in agreement with previous studies for small PMN supercells. The pair distribution function (PDF) of the 1:1 cell, resolved onto different atom types, is shown in Fig. 2. The PDF was obtained from the relaxed structure with a broadening of 0.03 a.u. The PDF is similar to that obtained by Grinberg and Rappe.[11] The first peak of Pb appears at 4.5 Å, with a width that is more diffused than those of Nb and Mg, reflecting larger Pb displacements. The magnitudes of the cation off-centerings with respect to centers of the O cages are given in Fig. 3. As may be seen the largest displacements are for Pb, reflecting the *A*-site driven nature of PMN. The average magnitude of the Pb off-centering, relative to the surrounding O cage is 0.51 Å. The displacements are noncollinear, so the magnitude of the average displacement is reduced to 0.43 Å, or in a ratio of 0.83. The Nb displacements are slightly larger than the Mg displacements, but are expected to be more important for the polar behavior because of the higher charge state and even higher Born charge on Nb relative to Mg.[13] The Nb and Mg displacements are also more collinear than the Pb displacements. The ratio of the magnitude of the average Nb displacement to the average magnitude of Nb displacement is 0.90. This ratio would be unity if the Nb displacements were

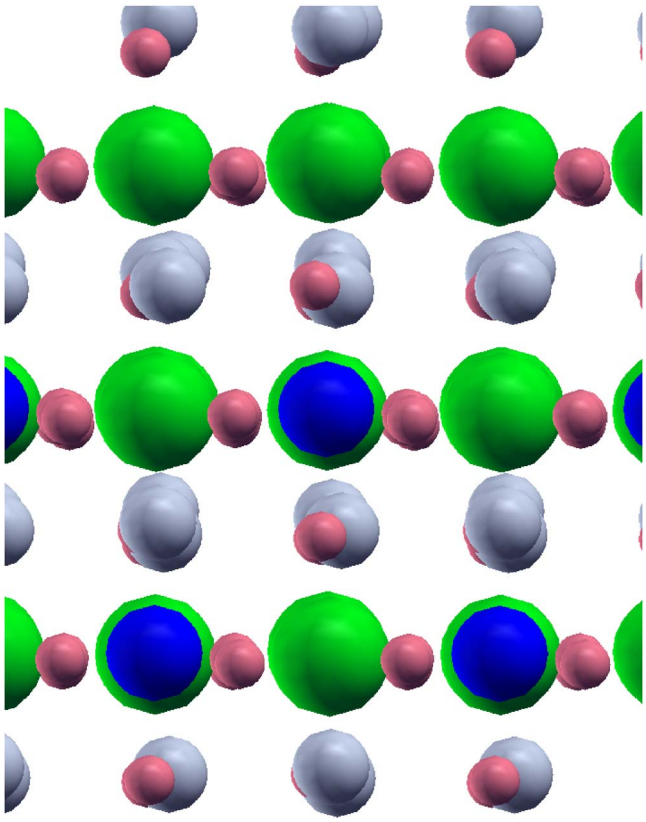

FIG. 1. (Color online) Structure of the 30 atom cell emphasizing the ordering of the Nb (large green) and Mg (large blue) atoms. O and Pb are shown as small pale red and grey spheres, respectively. The plot shown is a (110) view of the relaxed supercell.

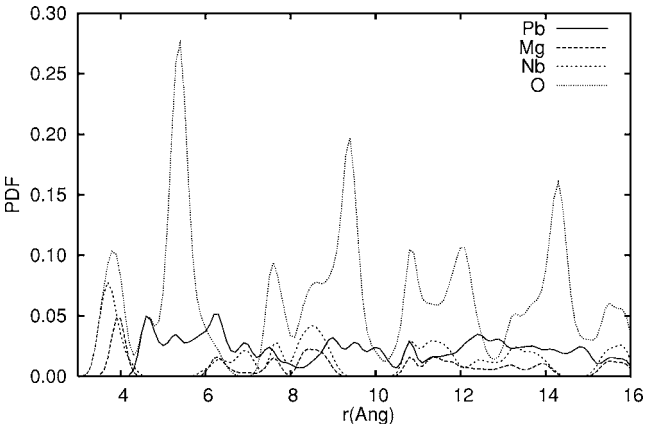

FIG. 2. Calculated pair distribution function for the relaxed 1:1 structure supercell, separated into Pb, Mg, Nb, and O contributions.

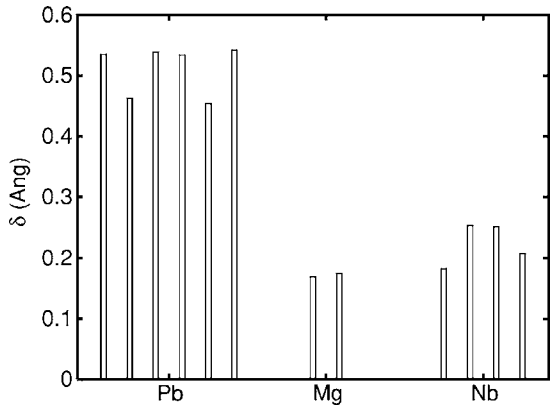

FIG. 3. Off-centering distance with respect to the octahedral oxygen cages for all Pb, Mg, and Nb in the 30 atom supercell. Note that these are the magnitudes of the off-centerings. The actual displacements are not collinear.

all collinear, and it would be zero if the directions of Nb displacements at different sites were uncorrelated, so that each Nb would have a displacement but the average displacement would be zero. As may be seen, besides noncollinearity, there are differences in the magnitudes of the off-centering among the different Pb and Nb atoms in the supercell. This is in accord with the previous findings of Grinberg and Rappe.[11]

The ratio of the smallest to the largest Pb off-centering in the supercell is 0.84. In an *A*-site driven material, one may assume that the *B*-site displacements are a response to *A*-site motion, both through short range bond competitions and the long range field. Regardless, since each *B*-site ion has six *A*-site neighbors, one would expect averaging, and so less variation in the *B*-site displacements. This is seen in the Mg displacements, but not in the Nb displacements. As mentioned, the Nb displacements are more collinear than the Pb displacements. However, the ratio of the smallest to largest Nb off-centering is 0.72. This is much smaller than the ratio for Pb, implying that some Nb sites are more active than others. If the interactions were purely local, and all Nb were equally active, the Nb displacement would be proportional to the average displacements of the eight nearest Pb neighbors, and the ratio of the Nb displacement to the average displacement of the nearest Pb neighbors would be constant. This is strongly violated, as shown in Table I.

IV. ELECTRONIC STRUCTURE

Figure 4 shows the electronic density of states (DOS) for the relaxed 30-atom supercell and projections onto unoccupied metal orbitals that might hybridize with O, specifically Pb *p*, Nb *d*, and Mg *d*. The O $2p$ valence bands extend from −5.3 eV to the valence band edge at 0 eV. The conduction bands are mainly Nb $4d$ derived near the band edge and become Pb $6p$ derived at higher energy, especially in the second main peak starting at ~5 eV. The unoccupied Mg *d* states are above the window plotted. The peak split off below the O $2p$ valence bands (this is the peak centered at ~−7 eV) is derived from the Pb $6p$ states. The expected result that there is no significant Mg *d* character in the valence bands is clearly seen. In addition, there is a noticeable Pb *p*character, distributed through the O *p* bands, and there is also considerable Nb *d* character concentrated at the bottom of the O *p* bands. This concentration reflects that primary crystal field splitting of the O $2p$ bands into p_σ (one per O) and p_π (two per O), due to hybridization with Nb, and that in spite of the importance of Pb-O hybridization for the polar character, Pb *p*-O *p* hybridization is not the strongest interaction for the purpose of the O crystal field. The main Nb-O hybridization is e_g-p_σ.

TABLE I. Atomic displacements of different Nb ions, *i*, with respect to the O cage (δ), magnitude of the average displacement of the nearest shell of Pb, with respect to the O cages around the respective Pb ions, δ_{Pb}, the ratio $r=\delta/\delta_{\mathrm{Pb}}$, $1s$ core level energy shift, E_{1s}, with respect to the average, *d*-*p* hybridization, $h_{p\text{-}d}$ measured by the integral of the Nb *d* projection of the DOS over the energy range of the O $2p$ bands, cage size, measured by the average Nb-O distance in the octahedra, d_{O}, and bond order *V*. N_{Nb} denotes the number of nearest *B*-site Nb neighbors.

i	N_{Nb}	δ (Å)	δ_{Pb} (Å)	*r*	E_{1s} (eV)	$h_{p\text{-}d}$	d_{O}(Å)	*V*
1	0	0.182	0.462	0.394	0.20	1.090	2.00	4.862
2	3	0.254	0.459	0.553	−0.01	1.107	2.01	4.868
3	3	0.251	0.460	0.546	−0.02	1.102	2.01	4.870
4	6	0.207	0.388	0.534	−0.17	1.111	2.01	4.870

In the 1:1 ordered supercell, there are two Nb sublattices. Nb ions on the mixed sublattice have only Nb *B*-site neighbors, while the Nb on the pure Nb sublattice have a mixture of Mg and Nb *B*-site neighbors. Considering the nominal charges of the ions, the expectation is that the potential on the mixed sublattice will be lower, favoring lower *d* bands and perhaps more hybridization. There are four Nb atoms in the 1:1 supercell that we studied. Of the Nb on the pure Nb sublattice, one has six Mg and no Nb nearest *B*-site neighbors (labeled "1" in the following), and the other two (labeled "2" and "3") have three Nb nearest *B*-site neighbors. The Nb on the mixed sublattice (labeled "4") has six Nb *B*-site neighbors. As may be seen from the $1s$ core level shifts (Table I), the Coulomb potential on sites with more Nb neighbors is lower, by ±0.2 eV around the average. This range of 0.4 eV is comparable to the upward shift of ~0.5 eV in the *d* bands in going from $KNbO_3$ to $KTaO_3$. The effect of this shift can be seen in the Nb *d* projections of the DOS. Figure 5 shows the projections for Nb on the pure and mixed sublattices. The onset of the main *d* DOS is shifted to higher energy for the pure Nb sublattice, following the Coulomb potential.

V. DISCUSSION AND CONCLUSIONS

One way to characterize the variation in O-Nb hybridization between different Nb sites is to use the integral of the Nb contribution to the valence density of states over the energy range of the O $2p$ bands. This varies over a 2% range among the different Nb sites, as given in Table I. Although

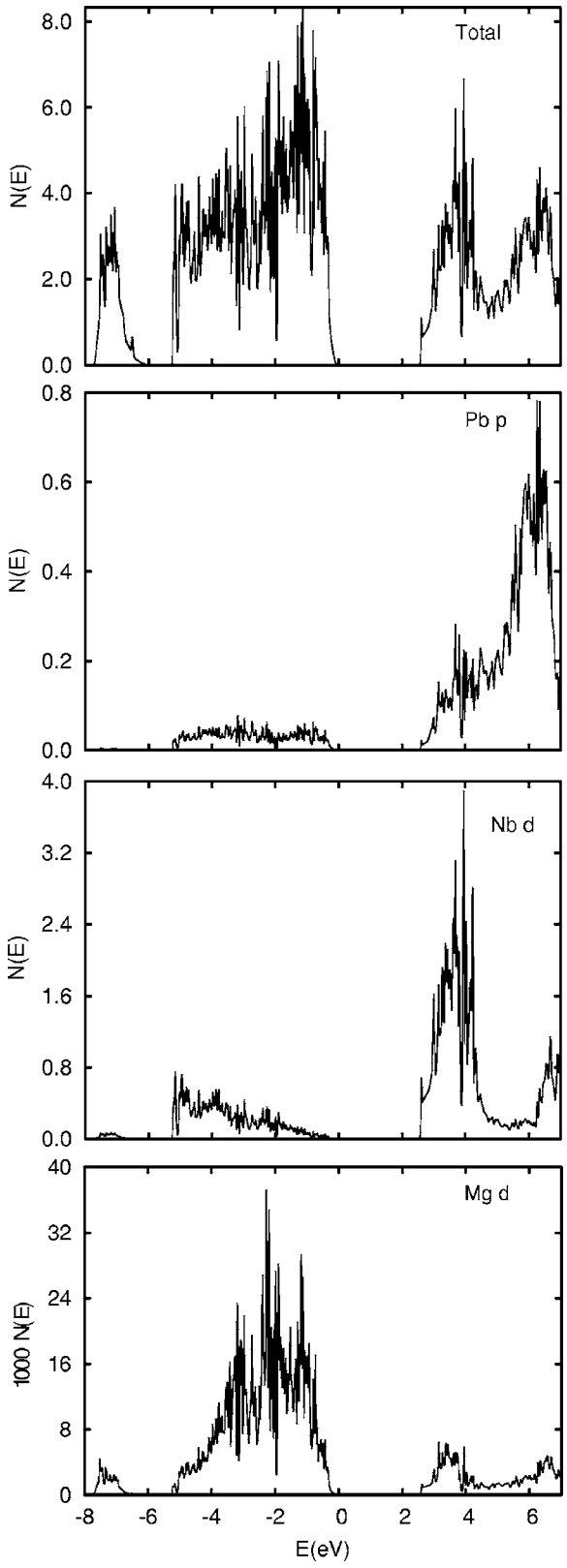

FIG. 4. Electronic density of states (top) and Pb p (second), Nb d (third), and Mg d (bottom) projections onto LAPW spheres for the relaxed 30 atom PMN supercell. The projections are on a per atom basis and the total DOS is per formula unit. Note the different vertical scales, especially that the Mg d projection is expanded by 1000.

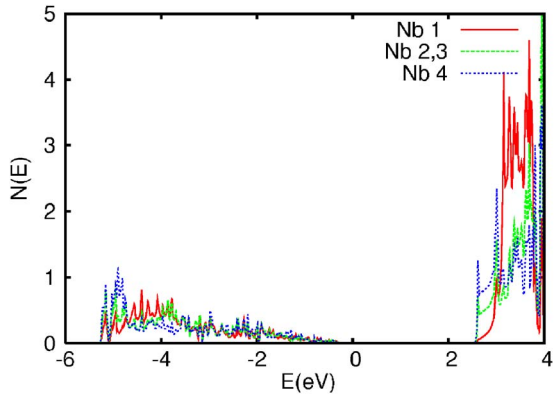

FIG. 5. (Color online) Site projected d DOS. Nb 1 has six Mg nearest B-site neighbors, Nb 2 and Nb 3 (the average is shown) have three Mg and three Nb neighbors, and Nb 4 has all Nb nearest neighbors.

this variation is small it follows the on-site Coulomb potential, measured by the core level shifts and the responsiveness of the Nb to the local Pb environment as measured by the ratio of the displacements, r. In particular, the Nb with only Mg neighbors are much less active than Nb with Nb neighbors. We note that in ferroelectric perovskites, there is a delicate balance between closed shell repulsions, Coulomb interactions, and hybridization, so that small changes can tip the balance.

Grinberg and co-workers have shown that bond competition is important in describing the structure of PMN and other perovskite solid solutions.[11,30,31] This competition can be quantified using bond valence criteria based on properties of the ions and the nearest neighbor distances.[32] In this approach, the bond order is expressed as a power law in bond distance R_{ij}. Each ion has a valence or total bond order which is a function of the bond distance[11,30,31] expressed as $V_i=\Sigma_j(R_{ij}/R^0)^{-N}$, where R^0 and N are empirical constants. For the four Nb sublattices, we used R^0 and N as 3.605 a.u. and 5, respectively.[32] Results are shown in Table I. Ideally, all ions have the same bond valence in a low energy structure, and this valence is close to the ideal value (5.0 for Nb).[11,30,31] It was also shown that besides being an indicator of favorable structures, this approach can be used to reproduce the shape of the energy surface in related materials.[30,33] Bond order also provides a mechanism for dependence of the site activity on the neighbor environment since motions of neighboring Nb ions will be coupled through bond competition with the shared O ion. Using the parameters above, we find that the bond order of all the Nb are very similar though lower than 5.0. We do not find a clear relationship between the on-site potential or the responsiveness of the Nb, and deviations of the bond orders in the relaxed structure from the ideal value, based on the present results. It may be that such a relationship, if present at all, is weak.

As mentioned, ferroelectric instabilities are typically strongly volume dependent.[16] This is the case for $KNbO_3$.[34] Thus it may be expected that Nb ions in compressed octahedra will show less off-centering than those in expanded octahedra. Table I also shows the cage sizes of the Nb, as characterized by the average Nb-O distance in the relaxed

structure. As may be seen, the variation in cage size among the different Nb sites is small, and cannot explain the different activities of the various Nb sites.

In conclusion, we have investigated the relationship between electronic structure and local displacements in a 1:1 ordered PMN supercell. In addition to trends emphasized previously, we find differences in the activity of different Nb sites depending on their local *B*-site coordination. These differences can be related to the on-site Coulomb potential, which affects the Nb *d*-O *p* hybridization.

ACKNOWLEDGMENTS

We are grateful for helpful discussions with D.I. Bilc, T. Egami, and I. Grinberg. This research is sponsored by the Department of Energy and the Office of Naval Research.

[1] G. Burns and F. H. Dacol, Solid State Commun. **48**, 853 (1983).
[2] J. Kuwata, K. Uchino, and S. Nomura, Jpn. J. Appl. Phys., Part 1 **21**, 1298 (1982).
[3] S. E. Park and T. R. Shrout, J. Appl. Phys. **82**, 1804 (1997).
[4] H. Fu and R. E. Cohen, Nature (London) **403**, 281 (2000).
[5] H. B. Krause, J. M. Cowley, and J. Wheatley, Acta Crystallogr., Sect. A: Cryst. Phys., Diffr., Theor. Gen. Crystallogr. **35**, 1015 (1979).
[6] N. Setter and L. E. Cross, J. Appl. Phys. **51**, 4356 (1980).
[7] V. Westphal, W. Kleemann, and M. D. Glinchuk, Phys. Rev. Lett. **68**, 847 (1992).
[8] H. You and Q. M. Zhang, Phys. Rev. Lett. **79**, 3950 (1997).
[9] R. Blinc, V. Laguta, and B. Zalar, Phys. Rev. Lett. **91**, 247601 (2003).
[10] B. P. Burton, E. Cockayne, and U. V. Waghmare, Phys. Rev. B **72**, 064113 (2005).
[11] I. Grinberg and A. M. Rappe, Phys. Rev. B **70**, 220101(R) (2004).
[12] S. A. Prosandeev, E. Cockayne, B. P. Burton, S. Kamba, J. Petzelt, Y. Yuzyuk, R. S. Katiyar, and S. B. Vakhrushev, Phys. Rev. B **70**, 134110 (2004).
[13] N. Choudhury, Z. Wu, E. J. Walter, and R. E. Cohen, Phys. Rev. B **71**, 125134 (2005).
[14] W. Zhong and D. Vanderbilt, Phys. Rev. Lett. **74**, 2587 (1995).
[15] R. E. Cohen, Nature (London) **358**, 136 (1992).
[16] G. A. Samara, Phys. Rev. B **1**, 3777 (1970).
[17] M. Fornari and D. J. Singh, Phys. Rev. B **63**, 092101 (2001).
[18] M. Ghita, M. Fornari, D. J. Singh, and S. V. Halilov, Phys. Rev. B **72**, 054114 (2005).
[19] D. J. Singh, Phys. Rev. B **53**, 176 (1996).
[20] D. J. Singh and L. Nordstrom, *Planewaves Pseudopotentials and the LAPW Method*, 2nd ed. (Springer, Berlin, 2006).
[21] D. Singh, Phys. Rev. B **43**, 6388 (1991).
[22] J. D. Pack and H. J. Monkhorst, Phys. Rev. B **13**, 5188 (1976); **16**, 1748 (1977).
[23] P. Blaha, K. Schwarz, G. K. H. Madsen, D. Kvasnicka, and J. Luitz, WIEN2K, an Augmented Plane Wave + Local Orbitals Program for calculating crystal properties (Karlheinz Schwarz, Technische Universitat Wien, Austria, 2002).
[24] E. Sjostedt, L. Nordstrom, and D. J. Singh, Solid State Commun. **114**, 15 (2000).
[25] Z. Wu, R. E. Cohen, and D. J. Singh, Phys. Rev. B **70**, 104112 (2004).
[26] M. D. Johannes and D. J. Singh, Phys. Rev. B **71**, 212101 (2005).
[27] G. Saghi-Szabo, R. E. Cohen, and H. Krakauer, Phys. Rev. Lett. **80**, 4321 (1998).
[28] J. P. Perdew, K. Burke, and M. Ernzerhof, Phys. Rev. Lett. **77**, 3865 (1996).
[29] P. Bonneau, P. Garnier, G. Calvarin, E. Husson, J. R. Gavarri, A. W. Hewat, and A. Morell, J. Solid State Chem. **91**, 350 (1991).
[30] I. Grinberg, V. R. Cooper, and A. M. Rappe, Nature (London) **419**, 909 (2002).
[31] I. Grinberg, V. R. Cooper, and A. M. Rappe, Phys. Rev. B **69**, 144118 (2004).
[32] I. D. Brown, *Structure and Bonding in Crystals* (Academic, New York, 1981).
[33] I. Etxebarria, J. M. Perez-Mato, A. Garcia, P. Blaha, K. Schwarz, and J. Rodriguez-Carvajal, Phys. Rev. B **72**, 174108 (2005).
[34] D. J. Singh and L. L. Boyer, Ferroelectrics **136**, 95 (1992).